Fall 8-17-2005

Antitrypanosomal, Antileishmanial, and Antimalarial Activities of Quaternary Arylalkylammonium 2-Amino-4-Chlorophenyl Phenyl Sulfides, a New Class of Trypanothione Reductase Inhibitor, and of N-Acyl Derivatives of 2-Amino-4-Chlorophenyl Phenyl Sulfide

Seheli Parveen

M. O. Faruk Khan
Marshall University, khanmo@marshall.edu

Susan E. Austin

Simon L. Croft

Vanessa Yardley

See next page for additional authors

Follow this and additional works at: http://mds.marshall.edu/sp_psr

Part of the Medicinal and Pharmaceutical Chemistry Commons, and the Pharmaceutics and Drug Design Commons

Recommended Citation

Parveen S, Khan MO, Austin SE, et al. Antitrypanosomal, antileishmanial, and antimalarial activities of quaternary arylalkylammonium 2-amino-4-chlorophenyl phenyl sulfides, a new class of trypanothione reductase inhibitor, and of N-acyl derivatives of 2-amino-4-chlorophenyl phenyl sulfide. J Med Chem 2005; 48(25): 8087-97.

Authors

Seheli Parveen, M. O. Faruk Khan, Susan E. Austin, Simon L. Croft, Vanessa Yardley, Peter Rock, and Kenneth T. Douglas

Antitrypanosomal, Antileishmanial, and Antimalarial Activities of Quaternary Arylalkylammonium 2-Amino-4-Chlorophenyl Phenyl Sulfides, a New Class of Trypanothione Reductase Inhibitor, and of *N*-Acyl Derivatives of 2-Amino-4-Chlorophenyl Phenyl Sulfide

Seheli Parveen,[†] Mohammed O. F. Khan,[†] Susan E. Austin,[†] Simon L. Croft,[‡,§] Vanessa Yardley,[‡] Peter Rock,[‡] and Kenneth T. Douglas*,[†]

School of Pharmacy and Pharmaceutical Sciences, University of Manchester, Oxford Road, Manchester M13 9PL, U.K., and London School of Hygiene and Tropical Medicine, Keppel Street, London WC1E 7HT, U.K.

Quaternization of the nitrogen atom of 2-amino-4-chlorophenyl phenyl sulfide analogues of chlorpromazine improved inhibition ∼40-fold (3′,4′-dichlorobenzyl-[5-chloro-2-phenylsulfanyl-phenylamino)-propyl]-dimethylammonium chloride inhibited trypanothione reductase from *Trypanosoma cruzi* with a linear competitive K_i value of 1.7 ± 0.2 μM). Molecular modelling explained docking orientations and energies by: (i) involvement of the Z-site hydrophobic pocket (roughly bounded by F396′, P398′, and L399′), (ii) ionic interactions for the cationic nitrogen with Glu-466′ or -467′. A series of *N*-acyl-2-amino-4-chlorophenyl sulfides showed mixed inhibition (K_i, K_i' = 11.3−42.8 μM). The quaternized analogues of the 2-chlorophenyl phenyl sulfides had strong antitrypanosomal and antileishmanial activity in vitro against *T. brucei rhodesiense* STIB900, *T. cruzi Tulahuan*, and *Leishmania donovani* HU3. The *N*-acyl-2-amino-4-chlorophenyl sulfides were active against *Plasmodium falciparum*. The phenothiazine and diaryl sulfide quaternary compounds were also powerful antimalarials, providing a new structural framework for antimalarial design.

Introduction

Major Third World tropical diseases, including African sleeping sickness, Chagas' disease, and leishmaniasis, are caused by pathogenic parasites of *Trypanosoma* spp. and *Leishmania* spp. The relatively few current treatments suffer from important drawbacks, and the need for new drugs is desperate; millions are currently at risk, and very many people die as a result of the lack of adequate therapies. Moreover, resistance against several of the available drugs has been reported.

A fundamental metabolic difference between mammalian host and trypanosomal or leishmanial parasite is the trypanothione redox-defense system.[1] In mammals, potential redox damage is dealt with by the glutathione (GSH)-based system during the course of which glutathione disulfide (**1**, GSSG) is formed. Regeneration of protective GSH from GSSG is catalyzed by glutathione reductase (GR). In trypanosomes and leishmanias, an analogous system has evolved[2] based on trypanothione, which as the disulfide (**2**, TSST) differs from GSSG by the spermidine cross-link between its two glycyl carboxyl groups. The enzyme trypanothione reductase (TR) reduces TSST to the dithiol form, analogously to GR. With this discovery, TR was quickly proposed as a target for the rational design of antitrypanosomal drugs,[1,3] a view supported by several subsequent proposals.[4−6] Trypanosomes do not contain GR,

but rather the analogous enzyme, TR, which does not accept GSSG as a substrate; conversely, host GR does not reduce TSST.[3,7] This mutually exclusive recognition and rejection of substrates between host and parasite enzymes suggested strongly that the selective-inhibitor design could be achieved.[3,4,7] TR has been shown genetically to be essential as TR-deficient *T. brucei* are nonvirulent and have raised susceptibilities toward oxidative stress.[8] Efficient selective blockade of TR would be expected to compromise the redox defenses of the parasites, increasing their sensitivity to redox-damage-based drugs, such as nifurtimox. Thus, a TR inhibitor might be a drug in its own right or when coadministered with a redox-active drug, such as nifurtimox, or perhaps even with synergy.[9]

During the course of these studies, we discovered that the target compounds not only showed marked antitrypanosomal and antileishmanial activities as was reasonable to expect on the basis of the target rationale used but that they were also active against the malarial parasite *Plasmodium falciparum*. To investigate this a little further, we initiated structure simplification to begin to define the pharmacophore for this unanticipated biological activity.

Following the early discovery of tricyclic inhibitors that are specific for TR over GR,[5] several classes of compounds have emerged to provide a framework on which to build TR inhibitors, including several families of tricyclics,[9−12] polyamine derivatives,[13−16] isoquinolines,[17] peptides,[18,19] and peptoids,[20] and there have been reviews of TR inhibition.[21−23]

The tricyclic neuroleptic framework[5,9,10] gives reasonably strong, selective inhibitors of TR, such as chlor-

* To whom correspondence should be addressed. Tel: 0161 275 2386. Fax: 0161 275 2481. E-mail: Ken.Douglas@man.ac.uk.
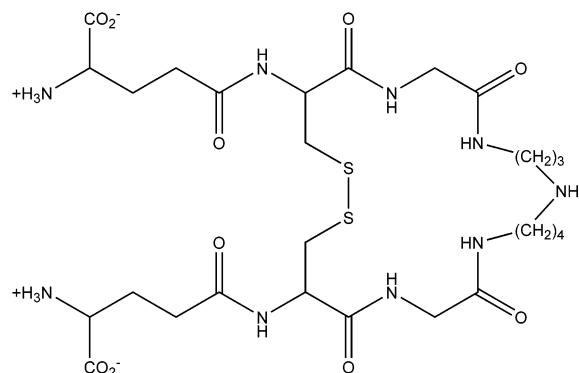† University of Manchester.
‡ London School of Hygiene and Tropical Medicine.
§ Present address: Drugs for Neglected Diseases Initiative, 1 Place St. Gervais CH-1202, Geneva.
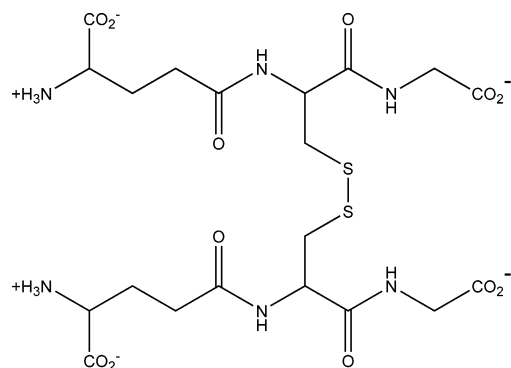
1, glutathione disulphide, GSSG

2, trypanothione disulphide, TSST

3, chlorpromazine

4, X = Cl, H

5

6

7

promazine (**3**), chlomipramine, amitryptyline, and trifluperazine, with K_i values of 10.8, 6.5, 93.6, and 23 μM, respectively. Ring-opening of the bridging site of the central ring gave inhibitors (such as **4**[9]), some of which were as powerful as more conformationally restricted analogues.
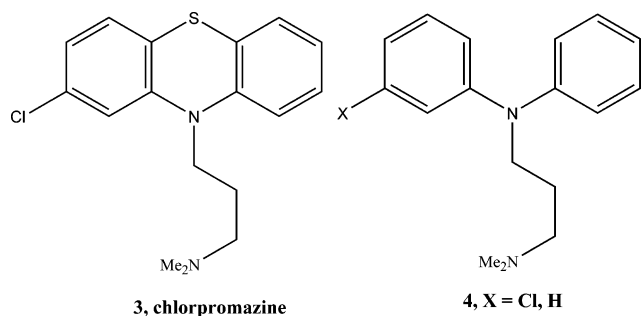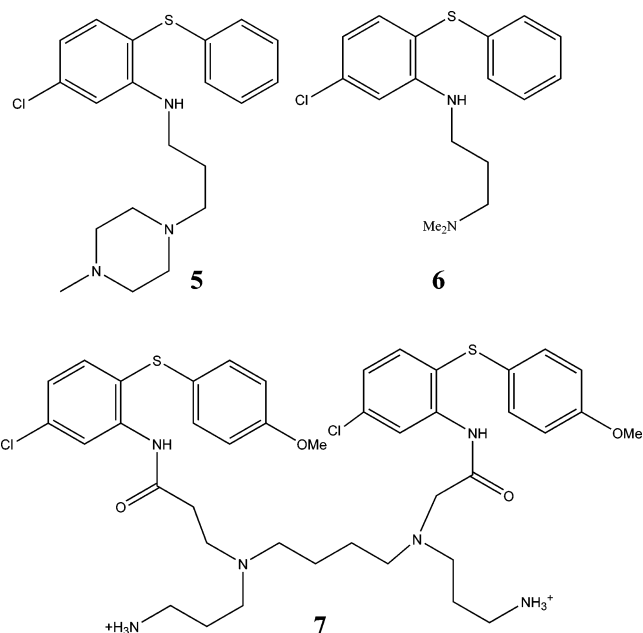
A series of diphenyl sulfides[24,25] also showed reasonably strong inhibition of TR (K_i values of 27 μM for **5** and 66 μM for **6**).[26] Modifications of the side chain by replacing the piperazine or dimethylamine with various linear or branched amine chains including spermine and spermidine yielded **7** ($I_{50} = 0.3 \mu$M) as the most potent TR inhibitor of this family.[24-27] Dimers of the 2-amino-diphenylsulfides also showed activity.[25] Some of these diphenyl sulfide open-chain analogues of chlorpromazine[24,25] show considerably lowered neuroleptic activity[26] and at 10^{-8} M led to weak or nonsignificant displacement in a binding study with the dopamine D_2 receptor using prochlorperazine as a control.[26]

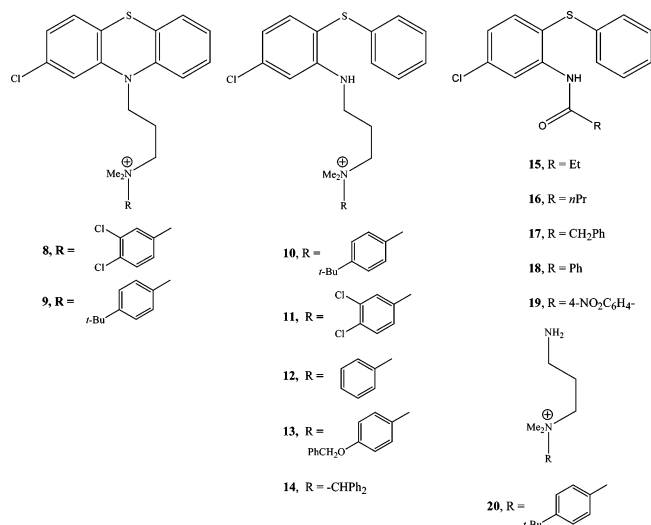TR can tolerate noncognate substrate architecture such as noncross-linked structures[28] and replacements of γ-glutamyl functions by hydrophobic structures,[29] the best being the benzyloxycarbonyl group.[29,30] Molecular modelling indicated[9] that the Z group of (ZCG·dmapa)$_2$ might make use of a hydrophobic pocket (the Z-site, approximately bounded by F396′, P398′, and L399′) not involved in binding the γ-glutamyl analogue (ECG.d-mapa)$_2$. Up to 2 orders of magnitude improvement in the binding strength of the parent phenothiazene tricyclics[5,9] could be achieved by a simple functionalization of the ω-terminus of the side chain on the central bridge nitrogen atom.[31] The rationale that led to this design improvement was to link the hydrophobic region putatively occupied by the tricyclic nucleus (M113, W21) with the Z-site. Appropriate hydrophobic quaternization of the tertiary amine produced strong inhibitors of *T. cruzi* TR (for example, K_i is 0.12 μM for **8** and 0.68 μM for **9**), and antiparasitic activity is retained.[31]

We now report the synthesis of some quaternary analogues (**10−14** and **20**) of open-chain compounds based on **6** along with details of their inhibition of *T. cruzi* TR and some preliminary antiparasite studies with them against *T. cruzi*, *T. b. rhodesiense*, *L. donovani*, and *P. falciparum*. The nature of some of the parasite-inhibition data was such that we sought to simplify the structures to begin to probe the minimal framework necessary to obtain strong antiparasite action. In doing so, we prepared compounds **15−19**, and their inhibition of *T. cruzi* TR is also reported.

Results

Synthesis. The quaternary alkylammonium derivatives of 2-amino-4-chlorophenyl phenyl sulfide were prepared (Scheme 1) similarly to the literature method[26] with some modifications; the overall yield was 54−61% based on the 2,5-dichloronitrobenzene or thiophenol. Using equimolar NaOH to activate the thiophenol, in contrast to metallic sodium,[26] gave higher yields (90%) and decreased the amounts of tarlike side products formed. Reduction of the nitro group carried out by means of iron/hydrochloric acid gave 86% yield (less convenient reduction by hydrazine hydrate in the presence of Raney-nickel (Raney-Ni) afforded the amine in

8, R =

9, R =

10, R =

11, R =

12, R =

13, R =

14, R = -CHPh₂

15, R = Et

16, R = nPr

17, R = CH₂Ph

18, R = Ph

19, R = 4-NO₂C₆H₄-

20, R =

96% yield). These methods are more convenient and cheaper than the literature method (high-pressure hydrogenation).

Inhibition by Quaternary Alkylammonium Chlorpromazines. A typical set of diagnostic plots, based on the combination of Lineweaver–Burk, Dixon, and Cornish-Bowden plots,[32] is shown for compound **8** in Figure 1. In agreement with data in a previous study,[31] at concentrations of inhibitor up to approximately 0.6 μM, the inhibition type appeared to be linear competitive with a K_i value of 0.18 ± 0.03 μM; these data are shown in Figure 1A. However, when the inhibitor

concentration range was increased to approximately 8 μM, the inhibition type was best analyzed as mixed inhibition, as shown in Figure 1B, with values of K_i = 0.44 ± 0.01 μM and K_i' = 3.5 ± 0.09 μM.

Compound **9**, studied only up to 20 μM because of solubility, gave linear competitive inhibition kinetics (Figure 2).

Inhibition by Quaternary Alkylammonium 2-Amino-4-chlorophenyl Phenyl Sulfides. The quarternary alkylammonium derivatives of 2-amino-4-chlorophenyl phenyl sulfide (**10**–**14**) were linear competitive inhibitors of *T. cruzi* TR, as can be seen in Figure 3 for compound **10**. Linear competitive inhibition kinetics were found for all of them at the concentrations used, and values of K_i using (ZCG·dmapa)₂ as a variable substrate are given in Table 1.

Inhibition by *N*-Acyl-2-amino-4-chlorophenyl Phenyl Sulfides. (*N*-Acyl-2-amino)phenyl sulfides (**15**–**19**) were mixed inhibitors of *T. cruzi* TR. Figure 4 shows a typical set of diagnostic plots for **16**. Values of K_i and K_i' collected in Table 2.

Inhibition by 2-Amino-4-chlorophenyl Phenyl Sulfide and by 20. 2-Amino-4-chlorophenyl phenyl sulfide was a weak mixed inhibitor (K_i = 0.15 ± 0.003 mM and K_i' = 0.86 ± 0.02 mM). Compound **20** was a very weak inhibitor and showed an I_{50} value of 0.60 ± 0.19 mM at 0.12 mM TSST under the standard assay conditions.

Biological Antiparasite Data. A number of the compounds were tested against *L. donovani*, *T. cruzi*, *T. b. rhodesiense*, and *P. falciparum*, and the results are
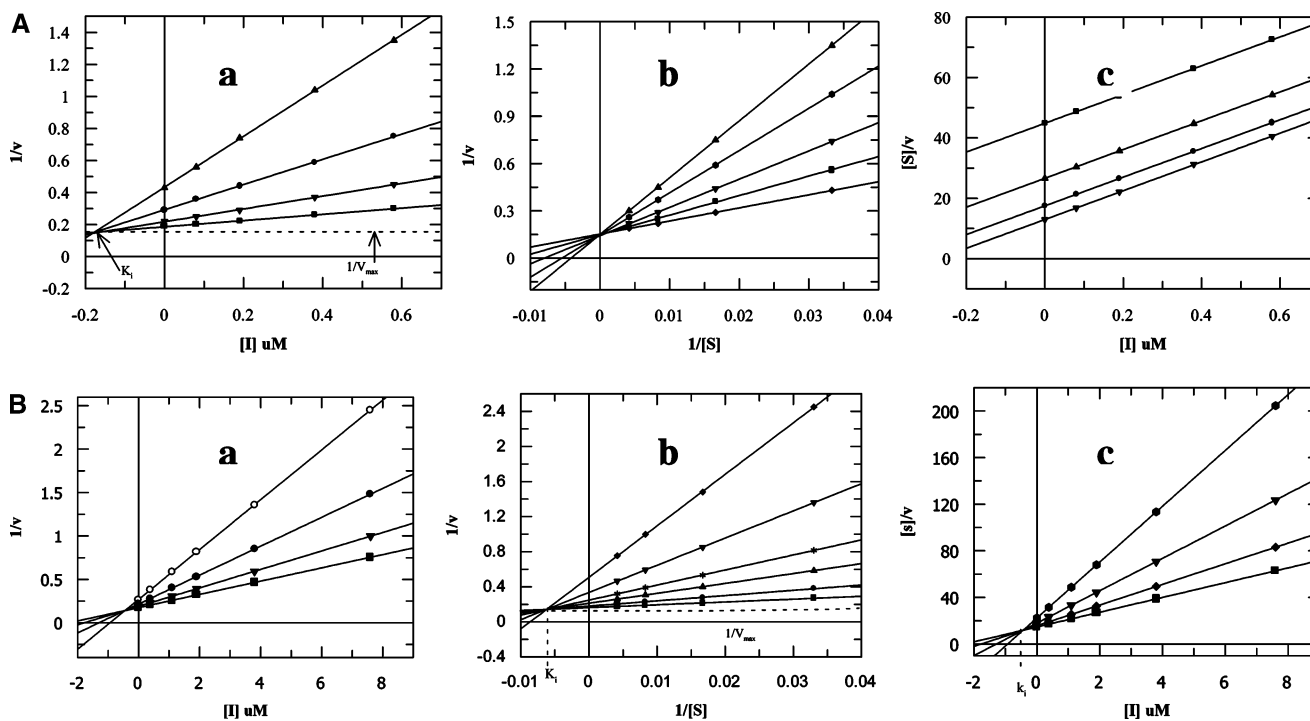
Figure 1. A: (a) Dixon plot (b) Lineweaver–Burk plot, and (c) Cornish-Bowden plot for inhibitor **8** at lower concentrations (0.08–0.58 μM) at pH 7.25, 25 °C in 0.02 M HEPES buffer containing 0.15 M KCl, 1 mM EDTA, 0.1 mM NADPH. Points are experimental, lines are theoretical, showing linear competitive inhibition with K_i = 0.18 ± 0.03 μM, V_{max} = 6.58 × 10⁻³ ΔA/s, and K_m = 55.3 ± 0.5 μM using TSST as variable substrate with S_1 = 30, S_2 = 60, S_3 = 120, and S_4 = 240 μM. Inhibitor concentrations used were I_1 = 0, I_2 = 0.08, I_3 = 0.19, I_4 = 0.38, and I_5 = 0.58 μM. B: (a) Dixon plot (b) Lineweaver–Burk plot, and (c) Cornish-Bowden plot for inhibitor **8** at pH 7.25, 25 °C in 0.02 M HEPES buffer containing 0.15 M KCl, 1 mM EDTA, 0.1 mM NADPH. Points are experimental, lines are theoretical for mixed inhibition with K_i = 0.44 ± 0.01 μM, K_i' = 3.5 ± 0.09 μM, V_{max} = 6.18 × 10⁻³ ΔA/s, and K_m = 19.8 ± 0.02 μM using TSST as variable substrate as S_1 = 30, S_2 = 60, S_3 = 120, and S_4 = 240 μM. The inhibitor concentrations used were I_1 = 0, I_2 = 0.38, I_3 = 1.1, I_4 = 1.9, I_5 = 3.8, and I_6 = 7.6 μM.

Figure 2. (a) Dixon plot (b) Lineweaver−Burk plot, and (c) Cornish-Bowden plot for inhibitor **9** at pH 7.25, 25 °C in 0.02 M HEPES buffer containing 0.15 M KCl, 1 mM EDTA, 0.1 mM NADPH. Points are experimental, lines are theoretical for linear competitive inhibition with $K_i = 0.57 \pm 0.03$ μM, $V_{max} = 9.08 \times 10^{-3}$ $\Delta A/$s, and $K_m = 40.4 \pm 0.02$ μM using TSST as variable substrate at $S_1 = 30$, $S_2 = 60$, $S_3 = 120$, and $S_4 = 240$ μM,. Inhibitor concentrations used were $I_1 = 0$, $I_2 = 2$, $I_3 = 5$, $I_4 = 10$, $I_5 = 15$, and $I_6 = 20$ μM.
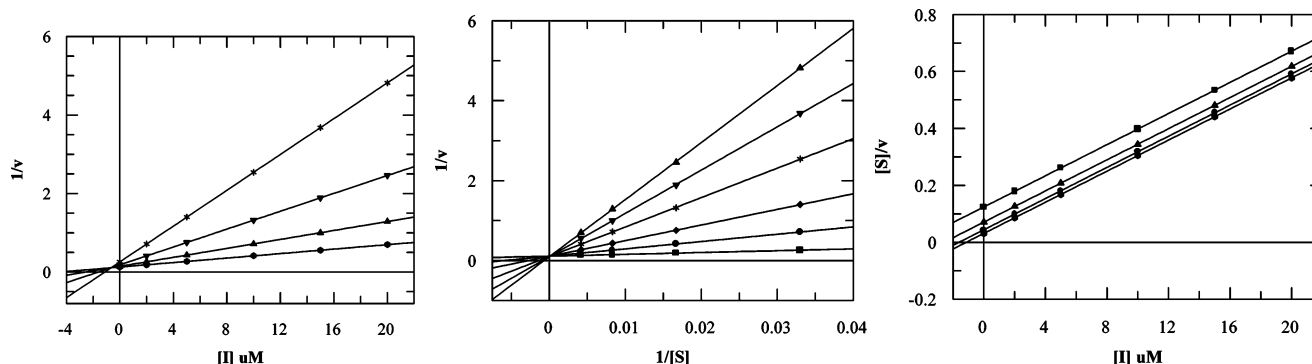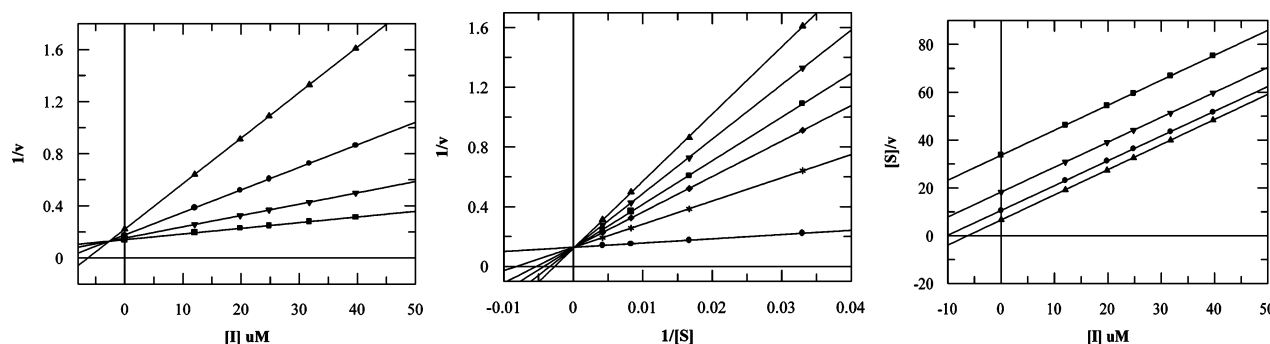

Figure 3. (a) Dixon plot (b) Lineweaver−Burk plot, and (c) Cornish-Bowden plot of inhibitor **10** at pH 7.25, 25 °C in 0.02 M HEPES buffer containing 0.15 M KCl, 1 mM EDTA, 0.1 mM NADPH using TSST as variable substrate at $S_1 = 30$, $S_2 = 60$, $S_3 = 120$, and $S_4 = 240$ μM. Points are experimental, lines are theoretical for linear competitive inhibition with $K_i = 2.67 \pm 0.09$ μM, $V_{max} = 7.72 \times 10^{-3}$ $\Delta A/$s, and $K_m = 21.34 \pm 0.8$ μM. Inhibitor **10** concentrations used were: $I_1 = 0$, $I_2 = 12.02$, $I_3 = 19.84$, $I_4 = 24.8$, $I_5 = 31.74$, and $I_6 = 39.7$ μM.

Table 1. Linear Competitive Inhibition by Quaternary Alkylammonium-Substituted-2-amino-4-chlorophenyl Phenyl Sulfides of *T. cruzi* Trypanothione Reductase (3 μg/mL) in 0.02 M HEPES Buffer pH 7.25, 25 °C, Containing 0.15 M KCl, 1 mM EDTA, 0.1 mM NADPH, 0.24, 0.12, 0.06, and 0.03 mM (ZCG·dmapa)$_2$[a]

cmpd	TR inhibition K_i (μM)	mean energy of top cluster (kcal mol^{-1})	% runs in top 10 clusters	% runs in top 20 clusters
9	66 ± 6[b]	−66.04	27	48
12	14.2 ± 0.12	−91.37	27	43
11	1.69 ± 0.22	−70.04	21	37
14	5.3 ± 0.92	−73.05	16	29
13	6.6 ± 0.4	−70.47	17	37
10	6.5 ± 0.7[c]	−69.92	20	36

[a] For **11**, no inhibition of human glutathione reductase was detectable at 0.5 mM. Also indicated are the results of docking calculations. [b] Literature value.[26] [c] Using TSST as variable substrate gave linear competitive $K_i = 2.67 \pm 0.09$ μM.

summarized in Table 3. Compounds **8** and **9**, with the parent phenothiazine quaternary structures, were selected because these substitution patterns had been shown in a previous study to confer strongest antitrypanosomal activity. Compound **10**, the ring-opened version of **8**, was also tested against this panel of parasites. The antitrypanosomal and antileishmanial activities of **8**−**10** were to be anticipated from previous studies,[31] but the powerful results in the test against *P. falciparum* that has been introduced as a standard part of this panel of tests were unexpected. On this

basis, the structurally simplified compounds **6** and **15**−**18** were tested (see Table 3).

Discussion

The data for these open-chain quaternaries can be compared with data for the parent compound, the open-chain analogue of chlorpromazine **9**, with a value [26] of $K_i = 66 \pm 6$ μM. The analogues in Table 1 provide evidence of improvement in the TR inhibition potency by 5−40-fold. Substitution with the simple aromatic ring (cf. **12** with **9**) gave ~5-fold improvement over the parent lead. For substitution by diphenylmethyl (**14**), benzyloxybenzyl (**13**), or 4-*tert*-butylbenzyl (**10**), the improvements in TR inhibitory potency were about 10−15-fold. The strongest inhibitor of this series was the 3,4-dichlorobenzyl-quaternized derivative (**11**), which shows an improvement of 39-fold over **9**. This 3,4-dichlorobenzyl substitution was also found to be optimal for the chlorpromazine quaternary systems.[31] This family of compounds shows clear evidence of inhibitory potency over the nonquaternized open-chain analogues of chlorpromazines.

These simple ring-opened variants of the quaternized compounds have two hydrophobic moieties. The major one is the "tricyclic" parent region (here an opened chain), which may interact with the major hydrophobic region corresponding to W21 and M113 of the enzyme active site in a way similar to that postulated [9,10] for chlorpromazine and other tricyclics. The second hydro-
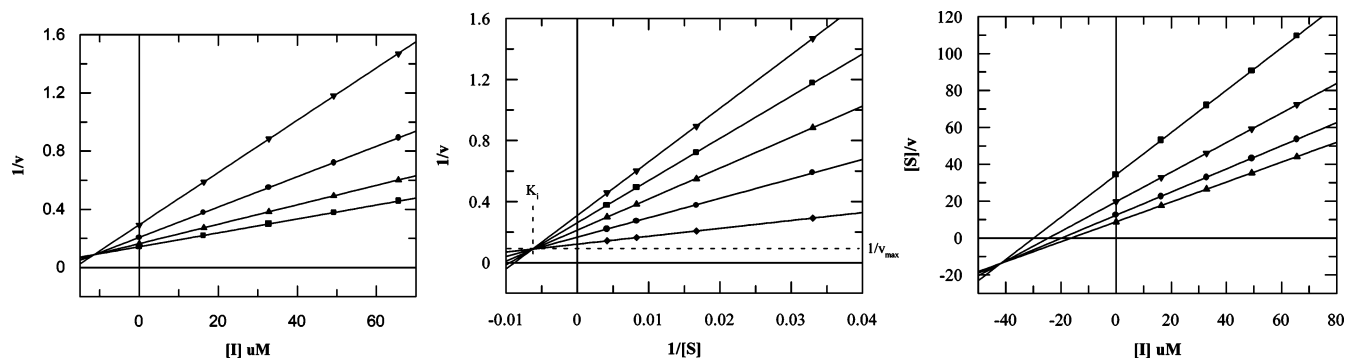
Figure 4. (a) Dixon plot (b) Lineweaver−Burk plot, and (c) Cornish-Bowden plot of inhibitor **16** at pH 7.25, 25 °C in 0.02 M HEPES buffer containing 0.15 M KCl, 1 mM EDTA, 0.1 mM NADPH. Points are experimental, lines are theoretical for mixed inhibition with $K_i = 11.3 \pm 0.5 \, \mu M$, $K_i' = 42.6 \pm 1.8 \, \mu M$, $V_{max} = 8.21 \times 10^{-3} \, \Delta A/s$, and $K_m = 42.08 \pm 1.3 \, \mu M$. The substrate (TSST) concentrations were 30, 60, 120, and 240 μM, and inhibitor **16** concentrations used were: $I_1 = 0$, $I_2 = 16.35$, $I_3 = 32.8$, $I_4 = 49.2$, and $I_5 = 65.6 \, \mu M$.

Table 2. Inhibition Data for Mixed Inhibition of *T. cruzi* Trypanothione Reductase by *N*-Substituted 2-Amino-4-chlorophenyl Sulfides at pH 7.25, 25 °C in 0.02 M HEPES Buffer Containing 0.15 M KCl, 1 mM EDTA, 0.1 mM NADPH with TSST as Variable Substrate

cmpd	$K_i (\mu M)$	$K_i' (\mu M)$	$IC_{50} (\mu M)$
15	20 ± 0.2	29.3 ± 0.13	31.6 ± 2.6
16	11.3 ± 0.5	42.6 ± 1.8	30.5 ± 0.14
17	24.6 ± 0.17	35.9 ± 0.09	36.8 ± 1.2
18	24.5 ± 0.09	37.7 ± 0.06	49.6 ± 3.4
19	42.8 ± 6	12.9 ± 1.7	44.5 ± 1.2

phobic moiety is formed by the benzyl or benzyl-substituted groups via quaternization of the propylamino side chain. These two hydrophobic regions of the inhibitor may be oriented in the TR active site by the ionic interactions formed by the positive charge of the inhibitor molecule (N^+) and the side chains of the glutamates (E466′ or 467′) of the TR active site. To probe this further, quantitative docking methods were undertaken.

Molecular Modelling for 10−14. Compounds **10−14** have additional flexibility with three extra torsions in each molecule compared to that of phenothiazines such as **9**, due to the open conformation of the main ring structures. Docking energies and cluster data for ligands of this family were determined by a protocol exactly comparable to that published for **9**[31](Table 1). The bound conformations again revealed the patterns of interactions previously detected[31]for phenothiazines such as **9** (viz. of the positive nitrogen (N^+) of the ligand with Glu-465′/466′ or Ser-14). However, the bridging NH group also influences potential electrostatic interactions and binding orientations in some cases, but the favored conformations remain of energy similar to those of phenothiazine docking. The modes of binding found[31] for the cationic phenothiazines were: [*Mode I(a)*] The N^+ atom interacts electrostatically with E466′ (or sometimes E467′), and the tricyclic moiety resides in the hydrophobic Z-site (F396′/P398′/L399′). [*Mode I(b)*] The N^+ atom interacts electrostatically with E466′ (or sometimes E467′), with the hydrophobic quaternary aromatic group in the Z-site. [*Mode I(c)*] The N^+ atom interacts electrostatically with E466′ (or sometimes E467′), with the hydrophobic quaternary aromatic groups apparently not interacting with TR. [*Mode II*] The N^+ atom interacts electrostatically with S14 (usually showing no hydrophobic interactions, but some-
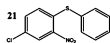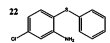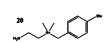
times with the tricyclic or benzyl-substituted group near the hydrophobic region of L17/W21/M113).

Compounds 6, 13, and 10 had roughly equal numbers of docked states in Modes I and II. For **9**, ~20% of the total 100 runs finished in Mode I and 25% in Mode II (the majority with the hydrophobic groups settling near L17W21/M113). In some of the conformations for both families, the NH group formed hydrogen bonds with nearby residues, e.g., −OH of Y110, E466′, and backbone carbonyl groups. For **13**, ~25% of the members of the top 20 clusters had the usual N^+−E465′/E466′ interaction, but usually with their hydrophobic groups lying in the open cavity of the active site. Another ~25% had the N^+−S14 interaction, some with the hydrophobic groups near W21/M113. Most of the other conformations had the ligand situated in the center of the cavity or toward the exterior away from protein residues. For **10**, a third of the conformations showed the N^+−E465′ interaction and one of the two hydrophobic groups docking near the Z-site or M113/L17/W21. About a third of the conformations had the usual interaction of N^+ with S14 and the benzyl group positioned near M113/L17. Other conformations only had the N^+−S14 or −E465′ interaction.

Compound 11. Three times as many final docked conformations were found with the N^+−S14 interaction as with the N^+−E465′ interaction. Only one significant cluster was seen (seven-members) with N^+−S14 and the hydrophobic sulfide atom in the Z-site. About the same number of conformations in other clusters also had N^+−S14 interactions but with the sulfur atom near the region containing W21/M113/Y110/L17. In some of these structures, the chlorine substituents on the benzyl group were within interacting distance of either E18 or E465′. Some other structures had a double N^+ and NH^- to E465′/E466′ interaction, or only the N^+−E465′ interaction.

Compounds 12 and 14. A very commonly detected docked conformation for these ligands was with the NH of the central ring interacting with E465′/466′ and the sulfide moiety (in the case of **12**) or the benzhydryl moiety (in the case of **14**) in the Z-site. This conformation accounted for half of the conformations for **12**. Many others had N^+−S14 interactions but no apparent hydrophobic interaction. Again, over half of the top low-energy conformations of **14** were positioned thusly, but

Table 3. Antiprotozoal Activities of 2-Amino-4-chlorophenyl Phenyl Sulfide, Its Quaternary Alkylammonium Analogues, and Its *N*-Acyl Derivatives[a,b,c]

Compound	Parasite	Percent inhibition							IC$_{50}$ (µg/mL)	Cytotoxicity (µg/mL)
		30	10	3.33	1.11	0.37	0.12	0.04		
8	*L. donovani* HU3	t/100	t/100	4.8	0				4	3.5
	T.cruzi Tulahuan	t/100	t/95.5	t/91.9	76.2				<1.1	
	T. b. rhodesiense STIB900	100	100	99	99.2	98.4	98.2	50.1	0.02	
	P.falciparum 3D7	100	99.6	99.7	98.4	30.4	20.4		0.47	
9	*L. donovani* HU3	t/100	t/+0	9.7	0				3.8	2.88
	T.cruzi Tulahuan	t/100	t/84.7	t/72.7	59.2				<1.1	
	T. b. rhodesiense STIB900	100	99.9	99.7	99.3	99.4	99.6	27.3	0.02	
	P.falciparum 3D7	100	99.7	99.6	99.6	34.1	11.7	0.44	0.13	
10	*L. donovani* HU3	t/100	t/100	7.4	0				3.9	2.14
	T.cruzi Tulahuan	t/97.4	t/86.9	t/61.5	t/79.1				<1.1	
	T. b. rhodesiense STIB900	100	100	99.2	99.4	99.1	99.3	60.9	0.01	
	P.falciparum 3D7	100	99.7	99.6	89	18.3	20.5		0.6	
15	*L. donovani* HU3	0							>30	93.1
	T.cruzi Tulahuan	71.8	24.6	0					18.3	
	T. b. rhodesiense STIB900	100	23.3	0					11.3	
	P.falciparum 3D7	26.9	0						>30	
16	*L. donovani* HU3	0							>30	>300
	T.cruzi Tulahuan	89.8	61.1	0					9.4	
	T. b. rhodesiense STIB900	97.8	15	9.6	0				14.2	
	P.falciparum 3D7	68.4	20.7	26	13.6				19.1	
17	*L. donovani* HU3	0							>30	>300
	T.cruzi Tulahuan	0							>30	
	T. b. rhodesiense STIB900	99.6	59.6	21.1	3.6				7.4	
	P.falciparum 3D7	50	45.4	69.3	8				30	
18	*L. donovani* HU3	0							>30	9
	T.cruzi Tulahuan	89.6	2.9	0					19.8	
	T. b. rhodesiense STIB900	99.6	57.4	7.4	20.7				8.7	
	P.falciparum 3D7	30.1	14.5	9.2	17.6				>30	
19	*L. donovani* HU3	0							>30	223
	T.cruzi Tulahuan	5.6	0						>30	
	T. b. rhodesiense STIB900	4.6	2.8	0					>30	
	P.falciparum 3D7	28.7	18.1	16.2	10.8				>30	
21 (structure)	*L. donovani* HU3	0							>30	43.1
	T.cruzi Tulahuan	91.3	41.4	0					11.3	
	T. b. rhodesiense STIB900	83.7	38.9	16.8	12.6				11.5	
	P.falciparum 3D7	93.4	14	4.3	4.1				15.6	
22 (structure)	*L. donovani* HU3	2.9	0						>30	47.9
	T.cruzi Tulahuan	89.4	81.6	22.8	15.5				6.7	
	T. b. rhodesiense STIB900	100	98.5	22.8	15.5				4.4	
	P.falciparum 3D7	95.4	39.4	13.5	2.5				11.3	
20 (structure)	*L. donovani* HU3	19.2	8.3						>30	>300
	T.cruzi Tulahuan	24	0	0	0				>30	
	T. b. rhodesiense STIB900	16.7	1.75	0					>30	
	P.falciparum 3D7	26.2	18.4	5.3	34.1				>30	

[a] KB screen for cytotoxicity. [b] *L. donovani* screen *t*/100 toxic to macrophages, no parasites present: *t*+0 toxic macrophages, parasites present. [c] *T. cruzi* screen *t/xx* toxic to macrophages/percent inhibition of parasite.

the N$^+$ was not seen to interact with any acidic residue or with S14 in any top cluster. The PhCH$_2$ group may sterically hinder binding to S14. The phenothiazine quaternized with the PhCH$_2$ group displayed a strong preference for the N$^+$ to bind E465′/466′, but **14** did not; the origin of this preference is not clear.

There was no correlation between the binding energies and the K_i values; for example, **11** is an 8-fold better

inhibitor than **12** on the basis of K_i values but binds less strongly from the docking study. Compound **6** did not bind differently with respect to docking energy or orientation to its quaternary derivatives and was docked in the N-protonated form.

Antiparasitic Activities. Antitrypanosomal and Antileishmanial Activities. Compound **5** at 27 μM has been reported to reduce the *T. cruzi* parasite number progressively over 12 h, whereas benznidazole and nifurtimox did not.[26] Compound **10** is an analogue of one of the most active quaternary chlorpromazines previously reported.[31] The data in Table 3 show that this ring-opened variant **10** is approximately as powerful against *T. cruzi* and *L. donovani* as the parent quaternized chlorpromazine **9**. However, it is twice as powerful against *T. b. rhodesiense*, showing very strong activity (IC$_{50}$ = 10 ng/mL). It showed some toxicity to KB cells but with a much higher IC$_{50}$ of 2.14 μg/mL, giving an efficacy to (this) toxicity ratio of 214. Signs of host macrophage toxicity also required similar higher levels in the *T. cruzi* ($\sim$1–3 μg/mL) and *L. donovani* ($\sim$10 μg/mL) tests. Thus, **10** represents a reasonable lead structure.

Removing the tricyclic structure or the dirayl sulfide moiety to give **20** effectively destroyed activity against all the parasites tested. The diaryl sulfide framework clearly had some inherent activity. Thus, against *T. cruzi*, **15**, **16**, **18**, **21**, and **22** showed IC$_{50}$ values in the range 6.7–19.8 μg/mL. The K_i values against TR for **15**–**19** were in the 10–40 μM range (mixed-type kinetics, Table 2). In contrast, **10**, with more powerful antiparasitic activity, showed a competitive K_i value of 6.5 μM (Table 1). Against *T. b. rhodesiense*, the IC$_{50}$ values of **15**–**18** and **21** and **22** ranged from 4.4 to 11.3 μg/mL, with **19** being essentially inactive. Against *L. donovani*, these compounds were inactive.

Antimalarial Activity. Unexpectedly, the ring-closed (tricyclic) quaternaries, **8** and **9**, clearly showed reasonably strong activity against the malarial parasite on the basis of the *P. falciparum* data in Table 3 (with IC$_{50}$ values against this strain of 0.47 and 0.13 μg/mL, respectively). This is not greatly affected (only 4-fold) by opening the central ring of the tricyclic to give **10**, for which the IC$_{50}$ value is 0.6 μg/mL. The *tert*-benzyl quaternary ammonium region of the molecule is clearly not the main activity determinant as the ID$_{50}$ value for **20** is >30 μg/mL. However, the other main region of the starting framework of **8** and **9**, viz. the amino-diaryl-sulfide moiety, does exhibit antiplasmodial activity with an ID$_{50}$ value of 11.3 μg/mL for **22**. Other evidence that this region provides an important part of the architecture of the pharmacophore comes from the activity of compound **16** (ID$_{50}$ = 19.1 μg/mL). Acylation generally leads to a loss of activity, but the *N*-propyl (**16**) is active. The amino group of **22** is not essential, given the similar activities of **21** and **22**.

A full structure-variation study remains to be done, but starting with the diaryl sulfide moiety, activity can be improved by incorporating the alkylamino-quaternary chain (**10**), which gives a 20-fold improvement in activity. Ring closure to give the tricyclic (**9**) improves activity a further 4-fold.

Phenothiazines have been mostly studied in malaria as adjuvants to chloroquine in chloroquine-resistant systems on the basis of their effects as MDR modulators, but they have also been reported to have intrinsic antimalarial activity,[33−36] which in some cases has been discussed in relation to their effects on β-hematin formation[37] and falcipain action to destroy hemoglobin.[38] The studies we report show that cationic versions of the phenothiazine nucleus are even more potent and thus may serve as leads. It has been suggested that, although chlorpromazine itself is unlikely to serve as the base for a new antimalarial, the thioridazine framework might.[35] The simplified nuclei based on diaryl sulfides reported here may be considered in the light of alternative targets in malaria.

Conclusion

The present work introduces the quaternized analogues of the 2-chlorophenyl phenyl sulfides as having strong antiparasite activity against trypansomes and leishmanias. ID$_{50}$ values as low as 10 ng/mL against *T. b. rhodesiense*, <1.1 μg/mL against *T. cruzi*, and 3.9 μg/mL against *L. donovani* were found. It also shows that the very simple molecular skeleton of diaryl sulfides has inherent activity against these parasites and this allows a different set of approaches to analogue optimization. The phenothiazine and diaryl sulfide quaternary compounds are also very powerful antimalarials with **9** having an IC$_{50}$ value against *P. falciparum* of 0.13 μg/mL. Even simplified structures such as the *N*-acyl diaryl sulfides retain intrinsic antiparasitic activities.

Experimental Section

Reagents were of the highest quality available and purchased from the suppliers indicated. Benzyl bromide, diphenylmethyl bromide, 4-(*tert*-butyl)benzyl bromide, borane−tetrahydrofuran complex anhydrous tetrahydrofuran, and anhydrous toluene, were purchased from Aldrich Chemical Co. as were 3,4-dichlorobenzyl chloride, bromodiphenylmethane and thiophenol. Fluka Chemicals Ltd. supplied 3-bromopropionyl chloride and Raney-Ni ready for use. Lancaster Synthesis supplied 2,5-dichloronitrobenzene and dimethylamine. Trypanothione disulfide was from Bachem or synthesized by a literature method,[39] GSSG and NADPH were from Boehringer, and *N*-benzyloxycarbonyl-L-cysteinylglycyl 3-dimethylaminopropyl amide disulfide was synthesized as described.[30]

Syntheses were monitored by thin-layer chromatography (TLC) on plastic sheets precoated to 0.2 mm with aluminum oxide (N/UV$_{254}$) (Merck, Darmstadt). The TLC solvent mixture used was A, chloroform:ethanol:acetic acid (10:9:1); B, diethyl ether:petroleum ether 40−60 (1:1); C, diethyl ether:petroleum ether 40−60 (1:9); D, diethyl ether:petroleum ether (2:8). R_f^X values indicate the solvent system used (X) as superscript. Spots were made visible by UV irradiation or by means of iodine vapor. Melting points were determined on a Reichert (Austria) melting point apparatus (Shandon Scientific Co. Ltd., London).

Values of pH were measured using a Corning 240 digital pH meter calibrated with standard buffers (Sigma) at 20 °C or using pH test strips (Sigma, range 0−14). All water used was distilled and purified by ion-exchange and charcoal filtering using a milliQ system (Millipore Ltd.). Phosphate, HEPES, and tris buffers were prepared from analytical reagent-grade materials according to standard procedures.

NMR spectra were recorded on a Jeol JNM EX 270 spectrometer operating at 270 MHz for ^{1}H NMR. Chemical shifts (δ) are reported in parts per million (ppm) relative to Me$_4$Si (0.00 ppm) as an internal reference. Data are reported using the following convention: chemical shift (integrated intensity, splitting patterns, assignment). Splitting patterns are abbrevi-

ated as: s, singlet; d, doublet; t, triplet; q, quartet; p, pentet; m, unresolved multiplet.

Fast-atom bombardment mass spectra (FAB-MS) were taken by means of a Kratos-Concept instrument operating in the FAB mode (Xe-beam bombardment) using *m*-nitrobenzyl alcohol (Aldrich Chemical Co.) as a matrix in the Department of Chemistry, University of Manchester. Elemental analyses were recorded on an EA 1108 Elemental Analyzer (Carlo Erba Instruments) in the Department of Chemistry, University of Manchester.

Enzyme Isolation, Assay, and Inhibition Studies. Trypanothione reductase from *T. cruzi* was isolated by means of overexpression of the gene in *Escherichia coli* JM109 cells bearing the expression vector PBSTNAV[40] as previously described.[5] The enzyme was homogeneous by the criterion of SDS-PAGE and had a specific activity identical to that of wild-type TR.[7] Enzyme activity was assayed at 25 °C in 0.02 M HEPES buffer, pH 7.25, containing 0.15 M KCl, 1 mM EDTA, 0.12 mM TSST, and 0.1 mM NADPH[7] at an enzyme concentration of approximately 0.3 μg/mL. For inhibition studies, TR assays were measured in 0.02 M HEPES buffer pH 7.25, 25 °C, containing 0.15 M KCl, 1 mM EDTA, 0.1 mM NADPH, 3 μg/mL TR, and varying concentrations of substrate ((ZCG·dmapa)$_2$) and inhibitor as indicated. For I_{50} determination, a single concentration of substrate (120 μM) was used. Human GR was isolated from an overexpression system for GR in *E. Coli* SG5 cells as described[41] and assayed following literature conditions[42] in 0.1 M potassium phosphate buffer, pH 7.00, containing 0.2 M KCl and 1 mM EDTA in the presence of 1 mM GSSG and 0.1 mM NADPH using approximately 15 μg/mL of GR per assay. Enzyme rate assays were conducted spectrophotometrically at 340 nm using a Peltier-thermostated cuvette holder maintained at 30.0 °C in a Cary 1E UV–visible spectrophotometer and using the Cary Enzyme Kinetics Software. Enzyme rate assays, spectral scans, and absorbance readings at fixed wavelengths were conducted spectrophotometrically using a Peltier-thermostated cuvette holder in a Cary 1E UV–visible spectrophotometer and using the Cary Enzyme Kinetics Software or using a Perkin-Elmer λ3B spectrophotometer thermostated with a Haake GH water circulator and attached to a Perkin-Elmer R100A chart recorder. Quartz cuvettes were used for readings in the UV range, for UV scanning of enzyme samples and compounds, and for determining extinction coefficients; otherwise, disposable plastic cuvettes were used.

Values of I_{50}, the concentration required to give 50% inhibition under the assay conditions described above, were determined by interpolation from a plot of assay velocity versus inhibitor concentration, fitting to the equation corresponding to linear competitive inhibition by nonlinear regression analysis written into Grafit. Inhibition type was assessed by analyzing the patterns of three diagnostic classes of plot: **1**/v_o versus **1**/[S_o] for various [**1**]; **1**/v_o versus [**1**] for various [S_o]; [S_o]/v_o versus [**1**] at various [S_o]. Values of K_i for competitive inhibition and of K_i and K_i' for mixed inhibition were determined by direct weighted (**1**/$v_o{}^2$ for weighting) least-squares nonlinear regression analysis of the raw data using the appropriate equation using the Grafit program (Erithacus Software, distributed by Sigma Chemical Co.), viz., for linear competitive inhibition, $v = V_{max}[S_o]/([S_o] + K_m(1 + [\mathbf{1}]/K_i))$, and for mixed inhibition, $v = V_{max}[S_o]/([S_o](1 + [\mathbf{1}]/K_i') + K_m(1 + [\mathbf{1}]/K_i))$. Values of V_{max} and K_m were obtained by least-squares nonlinear regression analysis using Grafit.

Parasitology. *Trypanosoma brucei rhodesiense.* STIB900 blood stream form (bsf) trypomastigotes were maintained in HMI-18 medium[43] with 15% heat-inactivated fetal calf serum (HIFCS) [Harlan-SeraLab, U.K.] at 37 °C, 5% CO$_2$/air mixture. Trypomastigotes were washed and resuspended in fresh medium at a concentration of 2×10^5/mL, and 100 μL was added to the drug dilutions. The top concentration for the test compounds was 30 μg/mL. The IC$_{50}$ for pentamidine is usually between 1.0 and 0.1 pg/mL. Plates were incubated for 72 h at 37 °C, 5% CO$_2$. At 72 h, the plates were assessed microscopically before Alamar blue was added.[44] Plates were read after

5–6 h on a Gemini fluorescent plate reader (Softmax Pro. 3.1.1, Molecular Devices, U.K.) at EX/EM 530/585 nm with a filter cutoff at 550 nm. IC$_{50}$ values were calculated with Ms*xl*fit (IDBS, U.K.)

Plasmodium falciparum. 3D7 (a chloroquine-sensitive strain) cultures were maintained in RPMI 1640 medium (Sigma, U.K.) 37 °C, 5% CO2 in 5% hematocrit. Asynchronous (65–75% ring stage) cultures were prepared at 0.5% parasitemia, and 50 L was added per well, the top test drug final concentration being 30 g/mL. After 24 h incubation, 37 °C, 5% CO2, 5 L of (3H)-hypoxanthine was added (0.2 Ci/well),[45,46] and plates were shaken for 1 min and then incubated for 48 h. The plates were freeze/thawed rapidly, harvested, and dried. Radioactive hypoxanthine uptake was measured by scintillation counter. IC$_{50}$ values were calculated using Ms*xl*fit.

Leishmania donovani. Peritoneal exudate macrophages were harvested from CD1 mice 24 h after starch induction. After washing, the macrophages were dispensed into Lab-tek 16-well tissue culture slides and maintained in RPMI1640 + 10% heat-inactivated fetal calf serum (HIFCS) at 37 °C, 5% CO$_2$/air mixture for 24 h. *Leishmania donovani* HU3 amastigotes were harvested from an infected golden hamster spleen and were used to infect the macrophages at a ratio of 5 parasites:1 macrophage. Amastigotes were counted using Thoma hemocytometer. Infected cells were left for a further 24 h and then exposed to the drug for a total of 5 days, with the overlay being replaced on day 3.[47] The top concentration for the test compounds was 30 μg/mL, and all concentrations were carried out in quadruplicate. The IC$_{50}$ value for the positive control drug, Pentostam, was usually 3–8 μg Sb^V/mL. On day 5, the overlay was removed, and the slides were fixed (100% methanol) and stained (10% Giemsa, 10 min) before being evaluated microscopically. IC$_{50}$ values were calculated using Ms*xl*fit.

Syntheses. The quaternary arylalkylammonium derivatives of 2-amino-4-chlorophenyl phenyl sulfide (**10**–**14**) were synthesized according to Scheme 1;[25] the preparation of 4-chloro-2-nitrophenyl phenyl sulfide and 2-amino-4-chlorophenyl phenyl sulfide used variants of literature methods[25] that are described here, whereas other steps followed literature protocols.

4-Chloro-2-nitrophenyl Phenyl Sulfide. 2,5-Dichloronitrobenzene (19 g, 0.1 mol) was added to a solution of thiophenol (11 g, 0.1 mol) in 5% ethanolic solution of NaOH (80 mL, 0.1 mol) and refluxed for 1 h, evaporated to dryness, and then dissolved in a mixture of ethyl acetate and water. The organic phase was dried with anhydrous Na$_2$SO$_4$ and evaporated to dryness under reduced pressure to give the crude product, which was then dissolved in a small amount of warm ethanol and left overnight at 4 °C to give yellow crystals, which were separated by filtration and washed with ethanol. The product was recrystallized from AcOH (26 g, yield 90%), $R_f{}^D$ 0.6; mp 82–83 °C (lit.[49] mp 81.5–84.5 °C).

2-Amino-4-chloro-phenyl Phenyl Sulfide. 4-Chloro-2-nitro-1-phenylsulfanyl-benzene (3 g, 11.3 mmol) was dissolved in warm ethanol (45 mL), and reduced iron powder (3.15 g, 56.5 mmol) was added. Concentrated hydrochloric acid (14 mL, 140 mmol) was added gradually and the reaction mixture refluxed for 1 h for the first two occasions (in the third instance, the reaction mixture turned colorless after adding concentrated hydrochloric acid, so reflux was omitted). Water was added to the reaction mixture, which was extracted twice with dichloromethane (2 × 10 mL). The combined organic layers were washed with dilute potassium carbonate solution (2 × 10 mL). The dichloromethane layer was collected, dried over anhydrous sodium sulfate, and evaporated to give a thick oily liquid from which the product was crystallized from its solution in cold methanol by the careful addition of cold water (2.3 g, 86% yield). An alternative procedure with Raney-Ni and hydrazine was as follows. A solution of 4-chloro-2-nitrophenyl phenyl sulfide (14.25 g, 0.05 mol) and 100% hydrazine hydrate (8 mL, 0.257 mol) in 225 mL of ethanol was heated to 50 °C, and about 2 g of Raney-Ni was added carefully (frothing occurs). When the initial frothing had subsided (after about 1

Scheme 1. Synthesis of Quaternary Alkylammonium (**10**) and *N*-Acyl (**15**−**19**) Derivatives of 2-Amino-4-chlorophenyl Sulfide[a]
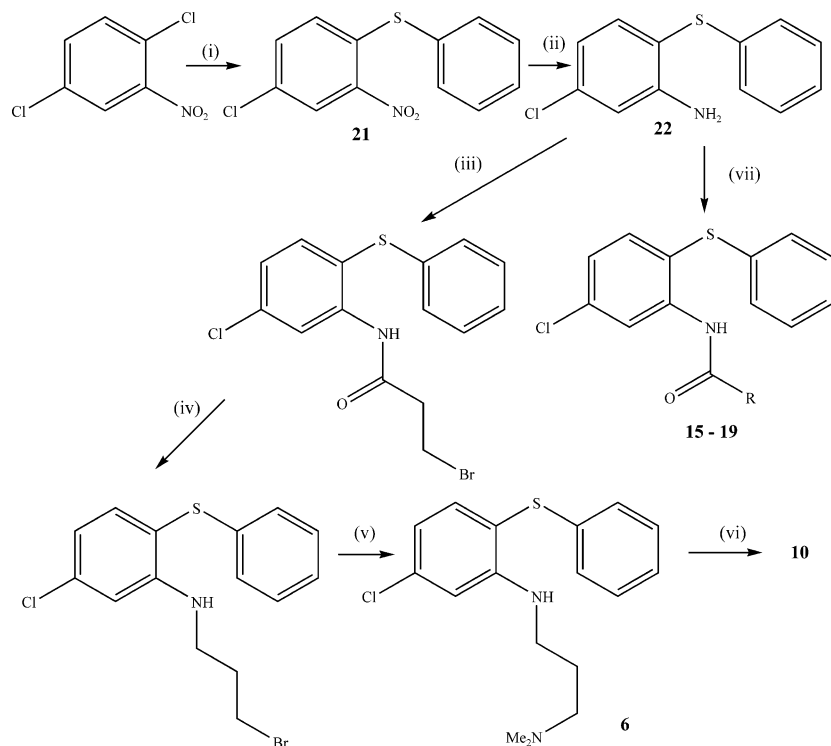
[a] (i) PhSH, 5% ethanolic NaOH, reflux, (ii) Fe/HCl in EtOH, (iii) 3-bromopropionyl chloride, dry CHCl$_3$, reflux, 30 min, (iv) BH$_3$·THF, (v) Me$_2$NH, Et$_3$N, toluene, reflux 16 H, (vi) alkyl halide, Me$_2$CO, overnight, (vii) RCOX/ Et$_3$N in CHCl$_3$

h), an additional 1 g of Raney-Ni was added and the mixture refluxed for 1 h. The catalyst was removed by filtration through Celite, solvent was evaporated under reduced pressure, and the product crystallized (12.7 g, yield 96%), R_f^D 0.75; mp 61−63 °C (lit.[49] mp 63−65 °C).

***N*-(3-Bromopropionyl)-5-chloro-2-phenylthiophenyl-amide).** The crude product was recrystallized from ethanol to yield the product quantitatively (7.8 g, 100%) as a colorless solid; R_f^B 0.5, mp 85−86 °C (lit.[25] mp 91 °C).

3-Bromo(*N*-(2-phenylthio-5-chloro)phenyl)propyl-amine was isolated (4.3 g, 79%) as a colorless semisolid. R_f^D 0.65; *m/z* (ES-MS): 355; δ_H (CDCl$_3$): 6.6−7.4 (8H, m, Ar), 6.6* (1H, t, broad, NH), 3−3.5 (4H, m, 2 × CH$_2$, attached to ring N and Br), 2.0 (2H, m, -CH$_2$-).

3-(*N*-(2-Phenylthio-5-chloro)phenyl) Propyldimethyl-amine was isolated quantitatively (3.1 g, 99%) as a yellowish oil. R_f^C 0.8; *m/z* (FAB-MS): 320; δ_H (CDCl$_3$): 7.4−6.6 (8H, m, Ph), 5.63* (1H, t, broad, NH), 3.15 (2H, q, CH$_2$−NHPh), 2.2 (2H, t, CH$_2$−NMe$_2$) 2.1 (6H, (CH$_3$)$_2$N), 1.7 (2H, p, -CH$_2$-).

Quaternary Arylalkylammonium 4-Chlorophenyl Phenyl Sulfides, (10−14). 3-Dimethylamino(*N*-(2-phenylthio-5-chloro)phenyl)propylamine (450 mg, 1.41 mmol) was dissolved in acetone (5 mL), and an equimolar amount of alkyl halide in acetone (5 mL) was added. The reaction mixture was stirred at room temperature for 18 h (for compound **10**, 3−4 days were needed to obtain a reasonable yield of product). The product precipitated (or ether was added to induce precipitation) and was collected by filtration, dried, and recrystallized from acetone−ether (yields were typically 80−90%). NMR spectral data and analytical data for the compounds **10**−**14** were satisfactory. The molecular weights of the compounds were estimated using fast atom-bombardment (Xe-beam) mass spectrometry, which gave the molecular ion (M$^+$) peak, usually as the most abundant peak (100%), with very low abundance peaks (5−25%) corresponding to the 3-dimethylamino(*N*-(2-phenylthio-5-chloro)phenyl)propylamine nucleus, the propylammonium side chain, and the 2-amino-4-chlorophenyl phenyl sulfide nucleus.

For quaternary alkylammonium derivatives of 2-amino-4-chlorophenyl phenyl sulfides **10**−**14**: **10**, Anal. (C$_{28}$H$_{38}$Cl$_2$N$_2$S) C, H, N; **11**, Anal. (C$_{24}$H$_{26}$N$_2$Cl$_3$BrS·1/2H$_2$O) C, H, N; **12**, Anal. (C$_{24}$H$_{28}$N$_2$ClBrS) C, H, N; **13**, Anal. (C$_{31}$H$_{34}$Cl$_2$N$_2$SO·H$_2$O) C, H, N; **14**, Anal. (C$_{30}$H$_{32}$ClBrN$_2$S) C, H, N.

For *N*-acyl derivatives of 2-amino-4-chlorophenyl phenyl sulfide **15**−**19**: **15**, Anal. (C$_{15}$H$_{14}$ClNOS) C, H, N; **16**, Anal. (C$_{16}$H$_{16}$ClNOS) C, H, N; **17**, Anal. (C$_{20}$H$_{16}$ClNOS) C, H, N; **18**, Anal. (C$_{19}$H$_{14}$ClNOS) C, H, N; **19**, Anal. (C$_{19}$H$_{13}$ClN$_2$O$_3$S) C, H, N.

Synthesis of Amide Derivatives of 5-Chloro-2-phenyl-sulfanyl-phenylamine. Amide derivatives of 5-chloro-2-phenylsulfanyl-phenylamine were synthesized according to Scheme 1 by standard acylation using the appropriate acid chloride.

Molecular Modelling Quantative Docking. Potential inhibitors were designed to bind via specific interactions: hydrogen bond, charge−charge, and hydrophobic. The published *Chamaecrista fasciculata*[6,50,51] and *T. cruzi*[52] X-ray diffraction coordinates were obtained from the Brookhaven database. Molecular modelling was carried out using Sybyl 6.4.2 software[53] and an R10000 or R4000 Silicon Graphics machine.

Docking searches, performed on a Silicon Graphics Origin 2000, took 12−76 hours CPU time using the program AU-TODOCK 2.4,[54] which uses a Metropolis Monte Carlo simulated-annealing for positional and configurational exploration with grids of molecular affinity potentials[55] based on the AMBER force field,[56] allowing the inclusion of terms for the Van der Waals', electrostatic, and hydrogen-bonding interactions. The X-ray structure of TR complexed with mepacrine[57] was used for docking studies. Mepacrine and all water molecules were removed, charged amines and carboxyl groups were capped, and essential hydrogens were added using the Kollman united-atom library. The X-ray structure was very briefly relaxed (25 steps Simplex) to remove any bad geometry and short contacts present, but not to allow any heavy atoms to move significantly from the calculated crystal structure positions. All ligands to be docked (Table 2) were built in SYBYL 6.4.2[53] with a formal charge of +1 added to the quaternary nitrogen atom. Partial atom-centered charges were calculated using the semi-empirical PM3 method implemented in MOPAC,[58] and after an initial

Simplex optimization, ligands were minimized to convergence (Powell method, gradient 0.05 kcal/mol).

The number of rotatable bonds of the ligands varies from 9 to 12; nonpolar hydrogens were united automatically using AUTOTORS. Using AUTOGRID, a grid (29.625 Å × 29.625 Å × 30.375 Å, with grid spacing 0.375 Å) was centered on the active site for each test case, with 40, 40, and 41 grid points in each Cartesian direction (80 points × 80 points × 82 points total per grid). Appropriate Lennard-Jones 12−10 parameters for H atoms bonded to O, N, or S in the ligand, and to O or S in the protein, were specified in the AUTOGRID parameter file (N atoms of TR were all assumed to participate in backbone amide bonds, making their lone pairs unavailable for hydrogen bonds).

As 50 docking runs of AUTODOCK performed for each ligand gave practically no clustering, 100 docking runs were carried out per docking. At the beginning of each simulated annealing run, the ligand was positioned randomly within the grid, and movement began with a random translation, random rigid body rotation, and random torsions. Each run consisted of 100 annealing cycles, a cycle terminating if the ligand made either 30 000 sequentially accepted or rejected moves. The annealing RT (616 cal mol^{-1} in the first cycle) was reduced linearly at the end of each cycle by 0.95-fold. The minimum energy state of the current cycle was used to start the next cycle. All cycles had a maximum translational step size of 0.2 Å and maximum torsional rotation of 5° per step.

Following docking, cluster analysis of all structures generated for a single compound was performed. Once sorted by total energy of interaction, the structures were sequentially assigned to cluster families, represented by top-of-cluster structures. Structures not satisfying a tolerance of 1.5 Å in the RMS deviation for all atoms to each top-of-cluster structure found defined new clusters. Each final docked position of mepacrine was referenced to that in the crystal structure. Ligand internal energy results were referenced to the initial undocked energy, calculated using AMBER. The calculated differences between the undocked and docked energies were used for analyses.

Appendix

Abbreviations. DMSO, dimethyl sulfoxide; GR, glutathione reductase; GSSG, glutathione disulfide; GSH, reduced glutathione; T[S]$_2$, trypanothione disulfide; T[SH]$_2$, reduced trypanothione as dithiol; TR, trypanothione reductase; HEPES, *N*-2-hydroxyethylpiperazine-*N'*-2-ethanesulfonic acid; THF, tetrahydrofuran; TEA, triethylamine; Z, benzyloxycarbonyl; (ZCG·dmapa)$_2$, *N,N*-bis-(benzyloxycarbonyl)-L-cysteinylglycyl-3-dimethylamino)propylamide disulfide.

Supporting Information Available: Analytical and spectral characterization data. This material is available free of charge via the Internet at http://pubs.acs.org.

References

(1) Fairlamb, A. H.; Blackburn, P.; Ulrich, P.; Chait, B. T.; Cerami, A. Trypanothione: A Novel Bis(glutathionyl)spermidine Cofactor for Glutathione Reductase in Trypanosomatids. *Science* **1985**, *227*, 1485−1487.
(2) Fairlamb, A. H.; Cerami, A. Metabolism and Functions of Trypanothione in the Kinetoplastida. *Annu. Rev. Microbiol.* **1992**, *46*, 695−729.
(3) Shames, S. L.; Fairlamb, A. H.; Cerami, A.; Walsh, C. T. Purification and Characterization of Trypanothione Reductase from *Crithidia fasciculata*, a New Member of the Family of Disulfide-Containing Flavoprotein Reductases. *Biochemistry* **1986**, *25*, 3519−3526.
(4) Schirmer, R. H.; Müller, J. G.; Krauth-Siegel, R. L. Disulfide-Reductase Inhibitors as Chemotherapeutic Agents: The Design of Drugs for Trypanosomiasis and Malaria. *Angew. Chem., Int. Ed. Engl.* **1995**, *34*, 141−154.
(5) Benson, T. J.; McKie, J. H.; Garforth, J.; Borges, A.; Fairlamb, A. H.; Douglas, K. T. Rationally Designed Selective Inhibitors of Trypanothione Reductase. *Biochem. J.* **1992**, *286*, 9−11.
(6) Hunter, W. N.; Bailey, S.; Habash, J.; Harrop, S. J.; Helliwell, J. R.; Aboagye-Kwarteng, T.; Smith, K.; Fairlamb, A. H. Active Site of Trypanothione Reductase. A Target for Rational Drug Design. *J. Mol. Biol.* **1992,** *227*, 322−333.
(7) Krauth-Siegel, R. L.; Enders, B.; Henderson, G. B.; Fairlamb, A. H.; Schirmer, R. H. Trypanothione Reductase from *Trypanosoma cruzi*: Purification and Characterization of the Crystalline Enzyme. *Eur. J. Biochem.* **1987**, *164*, 123−128.
(8) Krieger, S.; Schwarz, W.; Ariyanayagam, M. R.; Fairlamb, A. H.; Krauth-Siegel, R. L.; Clayton, C. Trypanosomes Lacking Trypanothione Reductase are Avirulent and Show Increased Sensitivity to Oxidative Stress. *Mol. Microbiol.* **2000**, *35*, 542−552.
(9) Chan, C.; Yin, H.; Garforth, J.; McKie, J. H.; Jaouhari, R.; Speers, P.; Douglas, K. T.; Rock, P. J.; Yardley, V.; Croft, S. L.; Fairlamb, A. H. Phenothiazine Inhibitors of Trypanothione Reductase as Potential Antitrypanosomal and Antileishmanial Drugs. *J. Med. Chem.* **1998**, *41*, 148−156.
(10) Garforth, J.; Yin, H.; McKie, J. H.; Douglas, K. T.; Fairlamb, A. H. Rational Design of Selective Ligands for Trypanothione Reductase from *Trypanosoma cruzi*. Structural Effects on the Inhibition by Dibenzazepines Based on Imipramine. *J. Enzyme Inhib.* **1997**, *12*, 161−173.
(11) Bonse, S.; Santelli-Rouvier, C.; Barbe, J.; Krauth-Siegel, R. L. Inhibition of *Trypanosoma cruzi* Trypanothione Reductase by Acridines: Kinetic Studies and Structure−Activity Relationships. *J. Med. Chem.* **1999**, *42*, 5448−5454.
(12) Bonse, S.; Krauth-Siegel, R. L.; Schlichting, I.; Lowe, G. Irreversible Inhibitors of *T. cruzi* Trypanothione Reductase: Kinetic and Crystallographic Studies. In *Flavins and Flavoproteins 1999, Proc. 13th Int. Symp Konstanz, Germany, August 29−September 4, 1999*; Ghisla, S., Kroneck, P., Macheroux, P., Sund, H., Eds; Agency for Scientific Publ.: Berlin, 1999.
(13) O'Sullivan, M. C.; Zhou, Q.; Li, Z.; Durham, T. B.; Rattendi, D.; Lane, S.; Bacchi, C. J. Polyamine Derivatives as Inhibitors of Trypanothione Reductase and Assessment of Their Trypanocidal Activities. *Bioorg. Med. Chem.* **1997**, *5*, 2145−2155.
(14) Li, Z.; Fennie, M. W.; Ganem, B.; Hancock, M. T.; Kobaslija, M.; Rattendi, D.; Bacchi, C. J.; O'Sullivan, M. C. Polyamines with *N*-(3-Phenylpropyl) Substituents Are Effective Competitive Inhibitors of Trypanothione Reductase and Trypanocidal Agents. *Bioorg. Med. Chem. Lett.* **2001**, *11*, 251−254.
(15) Ponasik, J. A.; Strickland, C.; Faerman, C.; Savvides, S.; Karplus, P. A.; Ganem, B. Kukoamine A and Other Hydrophobic Acylpolyamines: Potent and Selective Inhibitors of *Crithidia fasciculata* Trypanothione Reductase. *Biochem. J.* **1995**, *311*, 371−375.
(16) Chitkul, B.; Bradley, M. Optimizing Inhibitors of Trypanothione Reductase using Solid-Phase Chemistry. *Bioorg. Med. Chem. Lett.* **2000**, *10*, 2367−2369.
(17) Fournet, A.; Inchausti, A.; Yaluff, G.; Rojas De Arias, A.; Guinaudeau, H.; Bruneton, J.; Breidenbach, M. A.; Karplus, P. A.; Faerman, C. H. Trypanocidal Bisbenzylisoquinoline Alkaloids Are Inhibitors of Trypanothione Reductase. *J. Enzyme Inhib.* **1998**, *13*, 1−9.
(18) Garforth, J.; McKie, J. H.; Jaouhari, R.; Benson, T. J.; Fairlamb, A. H.; Douglas, K. T. Rational Design of Peptide-Based Inhibitors of Trypanothione Reductase as Potential Antitrypanosomal Drugs. *Amino Acids* **1994**, *6*, 295−300.
(19) McKie, J. H.; Garforth, J.; Jaouhari, R.; Chan, C.; Yin, H.; Besheya, T.; Fairlamb, A. H.; Douglas, K. T. Specific Peptide Inhibitors of Trypanothione Reductase with Backbone Structures Unrelated to That of Substrate: Potential Rational Drug Design Lead Frameworks. *Amino Acids* **2001**, *20*, 145−153.
(20) Chan, C.; Yin, H.; McKie, J. H.; Fairlamb, A. H.; Douglas, K. T. Peptoid Inhibition of Trypanothione Reductase as a Potential Antitrypanosomal and Antileishmanial Drug Lead. *Amino Acids* **2002**, *22*, 297−308.
(21) Austin, S. E.; Khan, M. A. O.; Douglas, K. T. Rational Drug Design using Trypanothione Reductase as a Target for Antitrypanosomal and Antileishmanial Drug Leads. *Drug Des. Discovery* **1999**, *16*, 5−23.
(22) Schmidt, A.; Krauth-Siegel, R. L. Enzymes of the Trypanothione Metabolism as Targets for Antitrypanosomal Drug Development. *Curr. Top. Med. Chem.* **2002**, *2*, 1239−1259.

(23) Augustyns, K.; Amssoms, K.; Yamani, A.; Rajan, P. K.; Haemers, A. Trypanothione as a Target in the Design of Antitrypanosomal and Antileishmanial Agents. *Curr. Pharm. Des.* **2001**, 7, 1117–1141.

(24) Baillet, S.; Buisine, E.; Horvath, D.; Maes, L.; Bonnet, B.; Sergheraert, C. 2-Amino Diphenylsulfides as Inhibitors of Trypanothione Reductase: Modification of the Side Chain. *Bioorg. Med. Chem.* **1996**, *4*, 891–899.

(25) Girault, S.; Baillet, S.; Horvath, D.; Lucas, V.; Davioud-Charvet, E.; Tartar, A.; Sergheraert, C. New Potent Inhibitors of Trypanothione Reductase from *Trypanosoma cruzi* in the 2-Aminodiphenylsulfide Series. *Eur. J. Med. Chem.* **1997**, *32*, 39–52.

(26) Fernandez-Gomez, R.; Moutiez, M.; Aumercier, M.; Bethegnies, G.; Luyckx, M.; Ouaissi, A.; Tartar, A.; Sergheraert, C. 2-Amino Diphenyldisulfides as New Inhibitors of Trypanothione Reductase. *Int. J. Antimicrob. Agents* **1995**, *6*, 111–118.

(27) Bonnet, B.; Soullez, D.; Davioud-Charvet, E.; Landry, V.; Horvath, D.; Sergheraert, C. New Spermine and Spermidine Derivatives as Potent Inhibitors of *Trypanosoma cruzi* Trypanothione Reductase. *Bioorg. Med. Chem.* **1997**, *5*, 1249–1256.

(28) Henderson, G. B.; Fairlamb, A. H.; Ulrich, P.; Cerami, A. Substrate Specificity of the Flavoproetin Trypanothione Disulfide Reductase from *Crithidia fasciculata*. *Biochemistry* **1987**, *26*, 3023–3027.

(29) El-Waer, A. F.; Smith, K.; McKie, J. H.; Benson, T. J.; Fairlamb, A. H.; Douglas, K. T. The Glutamyl Binding Site of Trypanothione Reductase from *Crithidia fasciculata*: Enzyme Kinetic Properties of Gamma-glutamyl-modified Substrate Analogues. *Biochim. Biophys. Acta* **1993**, *1203*, 93–98.

(30) El-Waer, A. F.; Douglas, K. T.; Smith, K.; Fairlamb, A. H. Synthesis of *N*-Benzyloxycarbonyl-L-cysteinylglycine 3-Dimethylaminopropylamide Disulfide: A Cheap and Convenient New Assay for Trypanothione Reductase. *Anal. Biochem.* **1991**, *198*, 212–216.

(31) Khan, M. O.; Austin, S. E.; Chan, C.; Yin, H.; Marks, D.; Vaghjiani, S. N.; Kendrick, H.; Yardley, V.; Croft, S. L.; Douglas, K. T. Use of an Additional Hydrophobic Binding Site, the Z Site, in the Rational Drug Design of a New Class of Stronger Trypanothione Reductase Inhibitor, Quaternary Alkylammonium Phenothiazines. *J. Med. Chem.* **2000**, *43*, 3148–3156.

(32) Dixon, M.; Webb, E. C. *Enzymes*; Academic Press: New York, 1979; p 155.

(33) Atamna, H.; Krugliak, M.; Shalmiev, G.; Deharo, E.; Pescarmona, G.; Ginsburg, H. Mode of Antimalarial Effect of Methylene Blue and Some of its Analogues on *Plasmodium falciparum* in Culture and Their Inhibition of *P. vinckei petteri* and *P. yoelii nigeriensis* in Vivo. *Biochem. Pharmacol.* **1996**, *51*, 693–700.

(34) Menezes, C. M. S.; Kirchgatter, K.; Di Santi, S. M.; Savalli, C.; Monteiro, F. G.; Paula, G. A.; Ferreira, E. I. In Vitro Chloroquine Resistance Modulation Study on Fresh Isolates of Brazilian *Plasmodium falciparum*: Intrinsic Antimalarial Activity of Phenothiazine Drugs. *Mem. Inst. Oswaldo Cruz* **2002**, *97*, 1033–1039.

(35) Gracio, M. A.; Gracio, A. J.; Viveiros, M.; Amaral, L. Since Phenothiazines Alter Antibiotic Susceptibility of Microorganisms by Inhibiting Efflux Pumps, Are These Agents Useful for Evaluating Similar Pumps in Phenothiazine-Sensitive Parasites? *Int. J. Antimicrob. Agents* **2003**, *22*, 347–351.

(36) Guan, J.; Kyle, D. E.; Gerena, L.; Zhang, Q.; Milhous, W. K.; Lin, A. J. Design, Synthesis, and Evaluation of New Chemosensitizers in Multi-Drug-Resistant *Plasmodium falciparum*. *J. Med. Chem.* **2002**, *45*, 2741–2748.

(37) Kalkanidis, M.; Klonis, N.; Tilley, L.; Deady, L. W. Novel Phenothiazine Antimalarials: Synthesis, Antimalarial Activity, and Inhibition of the Formation of *β*-Haematin. *Biochem. Pharmacol.* **2002**, *63*, 833–842.

(38) Dominguez, J. N.; Lopez, S.; Charris, J.; Iarruso, L.; Lobo, G.; Semenov, A.; Olson, J. E.; Rosenthal, P. J. Synthesis and Antimalarial Effects of Phenothiazine Inhibitors of a *Plasmodium falciparum* Cysteine Protease. *J. Med. Chem.* **1997**, *40*, 2726–2732.

(39) Kellam, B.; Bycroft, B. W.; Chhabra, S. R. Solid-Phase Applications of Dde and the Analogue Nde: Synthesis of Trypanothione Disulfide. *Tetrahedron Lett.* **1997,** *38*, 4849–4852.

(40) Meinnel, T.; Mechulam, Y.; Fayat, G. Fast Purification of a Functional Elongator tRNAmet Expressed from a Synthetic Gene in Vivo. *Nucleic Acids Res.* **1988**, *16*(16), 8095–8096.

(41) Nordhoff, A.; Bücheler, U. S.; Werner, D.; Schirmer, R. H. Folding of the Four Domains and Dimerization Are Impaired by the Gly446→Glu Exchange in Human Glutathione Reductase. Implications for the Design of Antiparasitic Drugs. *Biochemistry* **1993**, *32*, 4060–4066.

(42) Worthington, D. J.; Rosemeyer, M. A. Human Glutathione Reductase: Purification of the Crystalline Enzyme from Erythrocytes. *Eur. J. Biochem.* **1974**, *48*, 167–177.

(43) Hirumi, H.; Hirumi, K. Continuous Cultivation of *Trypanosoma brucei* Bloodstream Forms in a Medium Containing a Low Concentration of Serum Protein Without Feeder Cell Layers. *J. Antimicrob. Chemother.* **1989**, *75*, 985–989.

(44) Raz, B.; Iten, M.; Grether-Buhler, Y.; Kaminsky, R.; Brun, R. The Alamar Blue Assay to Determine Drug Sensitivity of African Trypanosomes (*T. b. rhodesiense* and *T. b. gambiense*) in Vitro. *Acta Trop.* **1997**, *68*, 139–147.

(45) O'Neill, M. J.; Bray, D. H.; Boardman, P.; Phillipson, J. D.; Warhurst, D. C. Plants as Sources of Antimalarial Drugs. Part. 1. In Vitro Test Method for the Evaluation of Crude Extracts from Plants. *Planta Med.* **1985**, 394–398.

(46) Desjardins, R. E.; Canfield, C. J.; Haynes, J. D.; Chulay, J. D. Quantitative Assessment of Antimalarial Activity in Vitro by a Semiautomated Microdilution Technique. *Antimicrob. Agents Chemother.* **1979**, *16*, 710–718.

(47) Neal, R. A.; Croft, S. L. An in Vitro System for Determining the Activity of Compounds Against the Intracellular Amastigote Form of *Leishmania donovani*. *J. Antimicrob. Chemother.* **1984**, *14*, 463–475.

(48) Buckner, F. S.; Verlinde, C. L. M. J.; la Flamme, A. C.; van Voorhis, W. C. Efficient Technique for Screening Drugs for Activity Against *Trypanosoma cruzi* using Parasites Expressing *β*-Galactosidase. *Antimicrob. Agents Chemother.* **1996**, *40*, 2592–2597.

(49) Loudon, J. D. Mobility of Groups in 3-Chloro-4-nitro and 5-Chloro-2-nitrophenyl Sulfones. *J. Chem. Soc.* **1939**, 902–904.

(50) Kuriyan, J.; Kong, X.-P.; Krishna, T. S. R.; Sweet, R. M.; Murgolo, N. J.; Field, H.; Cerami, A.; Henderson, G. B. X-ray Structure of Trypanothione Reductase from *Crithidia fasciculata* at 2.4-Å Resolution. *Proc. Natl. Acad. Sci. U.S.A.* **1991**, *88*, 8764–8768.

(51) Bailey, S.; Smith, K.; Fairlamb, A. H.; Hunter, W. N. Substrate Interactions Between Trypanothione Reductase and N¹-Glutathionylspermidine Disulphide at 0.28-nm Resolution. *Eur. J. Biochem.* **1993**, *213*, 67–75.

(52) Zhang, Y.; Bond, C. S.; Bailey, S.; Cunningham, M. L.; Fairlamb, A. H.; Hunter, W. N. The Crystal Structure of Trypanothione Reductase from the Human Pathogen *Trypanosoma cruzi* at 2.3 Å Resolution. *Protein Sci.* **1996**, *5*, 52–61.

(53) SYBYL 6.4.2.; Tripos Inc., 1998.

(54) Goodsell, D. S.; Morris, G. M.; Olson, A. J. Automated Docking of Flexible Ligands: Applications of AutoDock. *J. Mol. Recognit.* **1996**, *9*, 1–5.

(55) Goodford, P. J. A Computational Procedure for Determining Energetically Favorable Binding Sites on Biologically Important Macromolecules. *J. Med. Chem.* **1985**, *28*, 849–857.

(56) Weiner, S. J.; Kollman, P. A.; Case, D. A.; Singh, U. C.; Ghio, C.; Alagona, G.; Weiner, P. K. A New Force Field for Molecular Mechanical Simulation of Nucleic Acids and Proteins. *J. Am. Chem. Soc.* **1984**, *106*, 765.

(57) Jacoby, E. M.; Schlichting, I.; Lantwin, C. B.; Kabsch, W.; Krauth-Siegel, R. L. Crystal Structure of the *Trypanosoma cruzi* Trypanothione Reductase·Mepacrine Complex. *Proteins* **1996**, *24*, 73–80.

(58) Stewart, J. J. P. MOPAC: A Semiempirical Molecular Orbital Program. *J. Comput.-Aided Mol. Des.* **1990**, *4*, 1–105.